Strain Sensor Based on Flexible Polyimide Ionogel for Application in High- and Low-Temperature Environments

Shuangfei Xiang, Shuangshuang Chen, Mengting Yao, Feng Zheng and Qinghua Lu

School of Chemical Science and Engineering, Tongji University, Shanghai, 200092, China

Correspondence to: Qinghua Lu (E-mail: 16155@tongji.edu.cn)

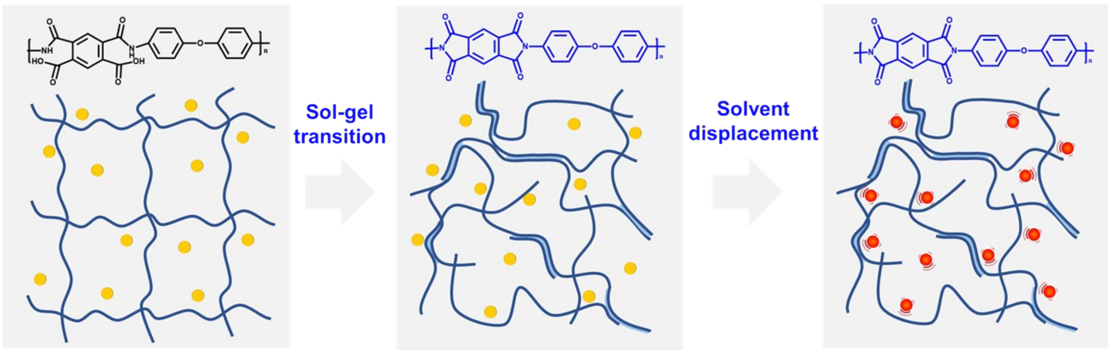

Figure S1. Scheme of gelation progress and solvent displacement.

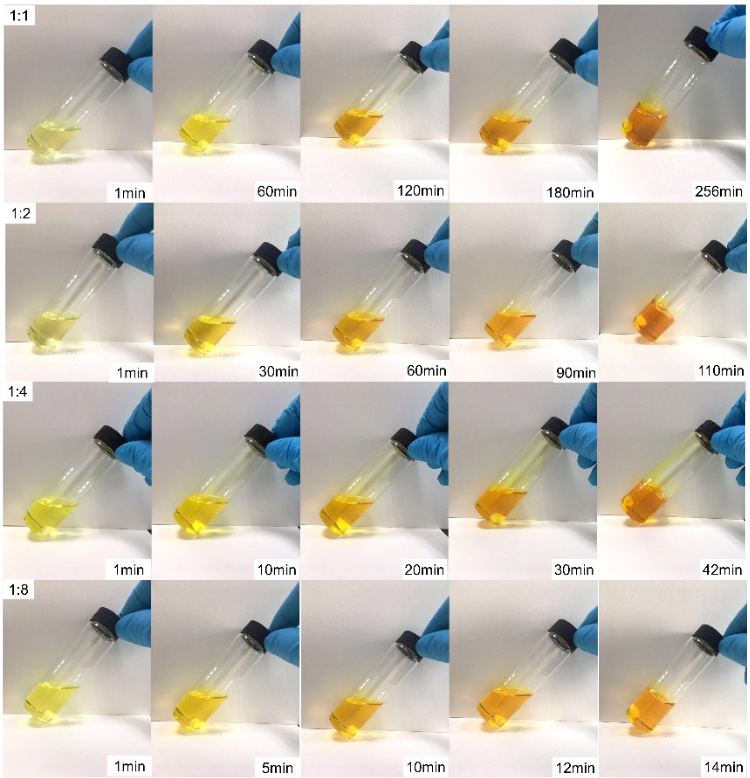

Figure S2. Optical images showing gelation progress of PAA after adding different contents of chemical imidization reagents (mole ratio of $M_{\text{pyridine}}/M_{\text{ODA}}$ was increased from 1/1 to 8/1).

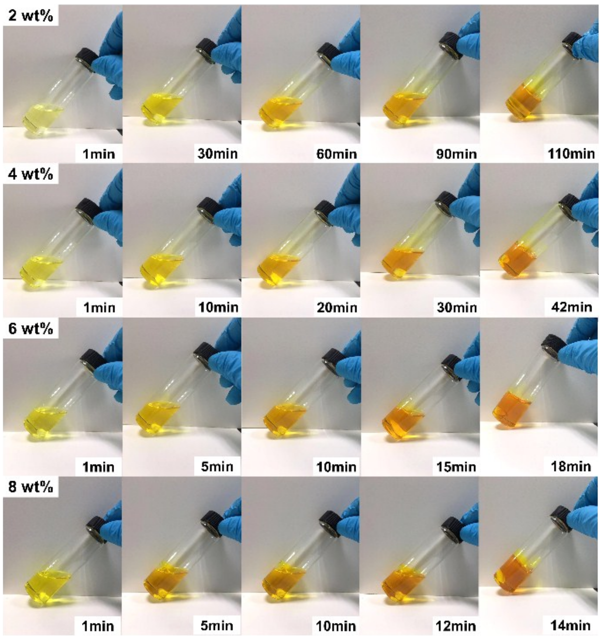

Figure S3. Optical images showing gelation progress of PAA after adding chemical imidization reagent. ($M_{\mathrm{pyridine}}/M_{\mathrm{ODA}}$ was fixed at 4/1, gelation time could be tuned by the PAA concentration from 2 wt%–8 wt%).

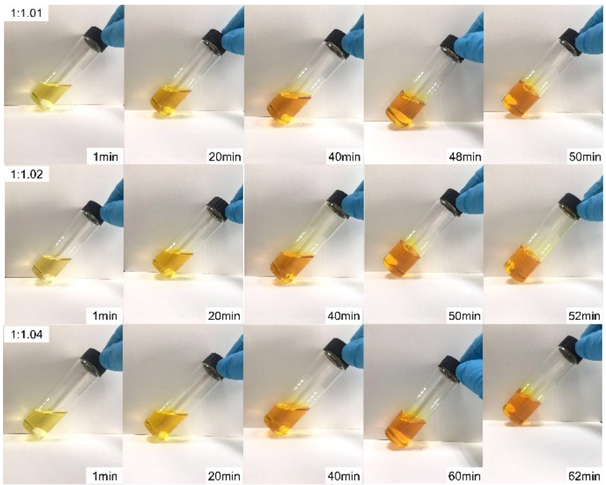

Figure S4. Three PAAs with different molecular weights synthesized by varying mole ratio of $M_{\mathrm{PMDA}}/M_{\mathrm{ODA}}$. When $M_{\mathrm{PMDA}}/M_{\mathrm{ODA}}$ was increased from 1.01 to 1.04, the corresponding molecular weight decreased from 2.2×10^4 to 1.1×10^4. Optical images showed gelation progress of PAA with different molecular weights after adding chemical imidization reagent (C_{PAA} and $M_{\mathrm{pyridine}}/M_{\mathrm{ODA}}$ fixed at 4 wt% and 4/1, respectively).

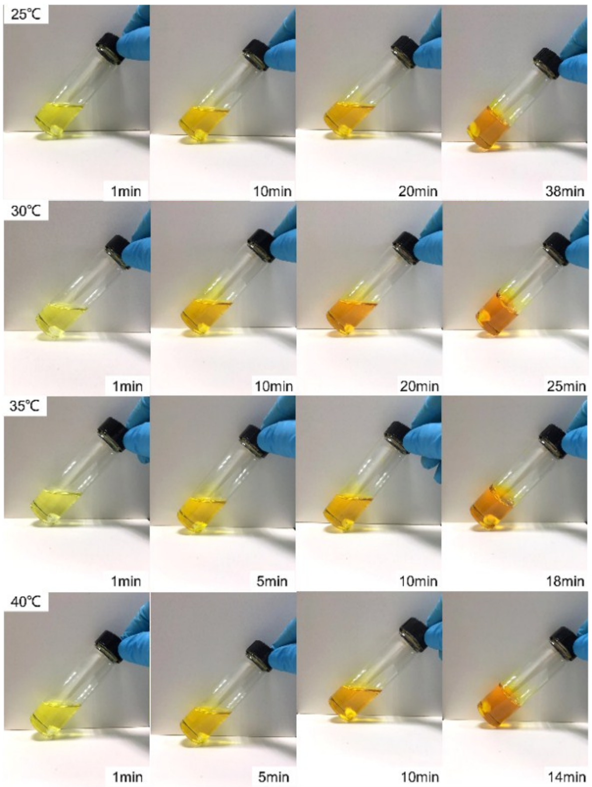

Figure S5. Optical images showing gelation progress of PAA after adding chemical imidization reagents in different ambient temperatures (C_{PAA} and $M_{pyridine}/M_{ODA}$ were fixed at 4 wt% and 4/1, respectively).

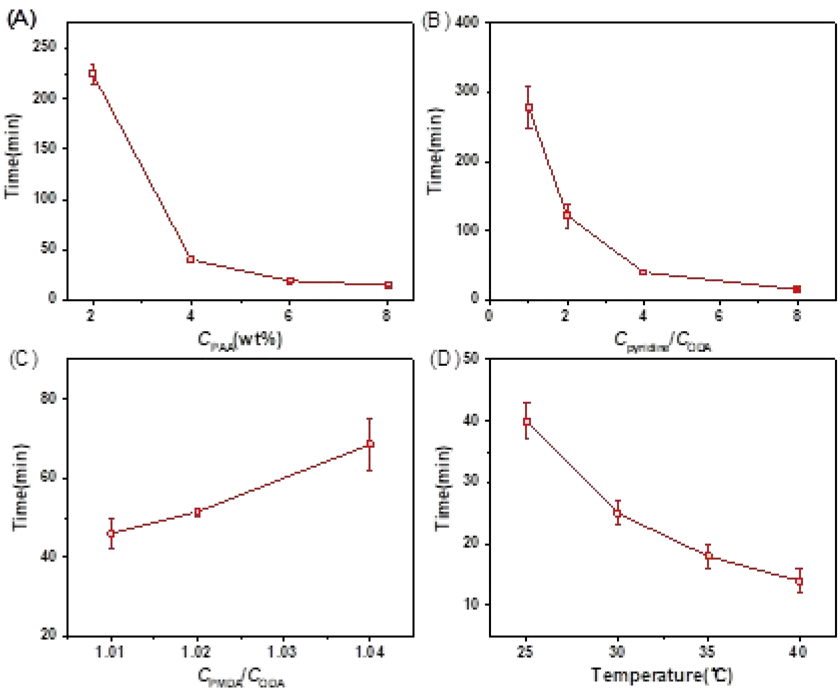

Figure S6. Relationship between gelation time and concentration of PAA (A), chemical imidization reagent (B), molecular weight of PAA (C) and chemical imidization temperature (D).

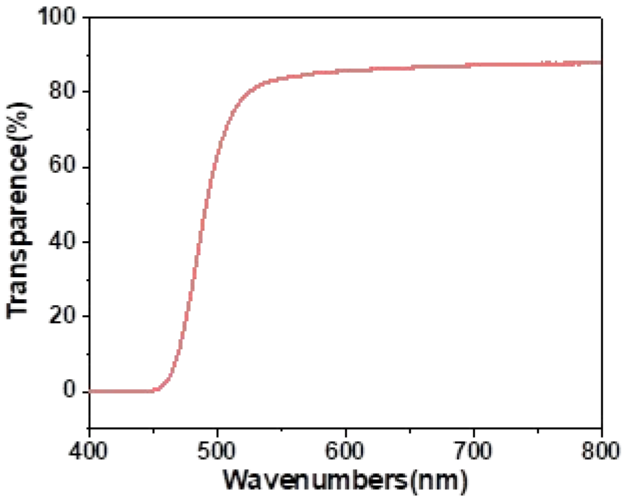

Figure S7. UV spectrum of polyimide ionogel.

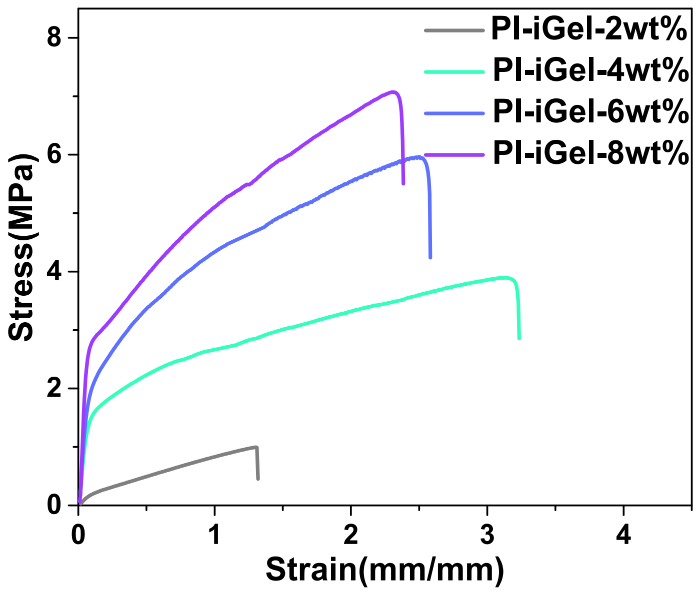

Figure S8. The stress-strain curves of PI-iGel

The impedance measurements were taken at -60℃ over a frequency from 100 kHz to 10 mHz. The conductivity of the PI iGel is estimated according to the following equation:

$$\sigma = L/(S \cdot R)$$

where L is the thickness of the ionogel, S is the area of the electrode. The bulk resistance of the ionogel, R, can be calculated from the fitting procedure.

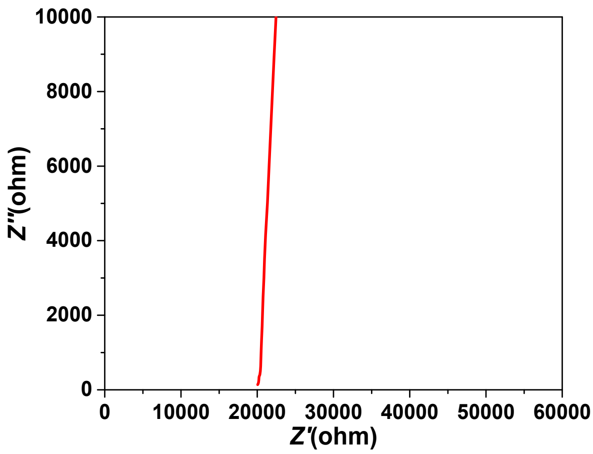

Figure S9. Impedance spectra for PI iGel at -60℃.

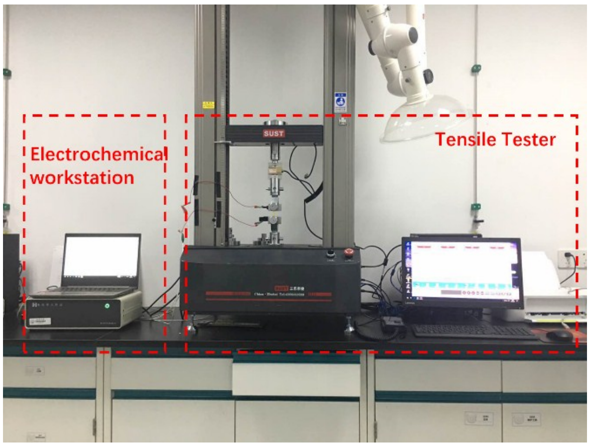

Figure S10. Test system for strain-current test

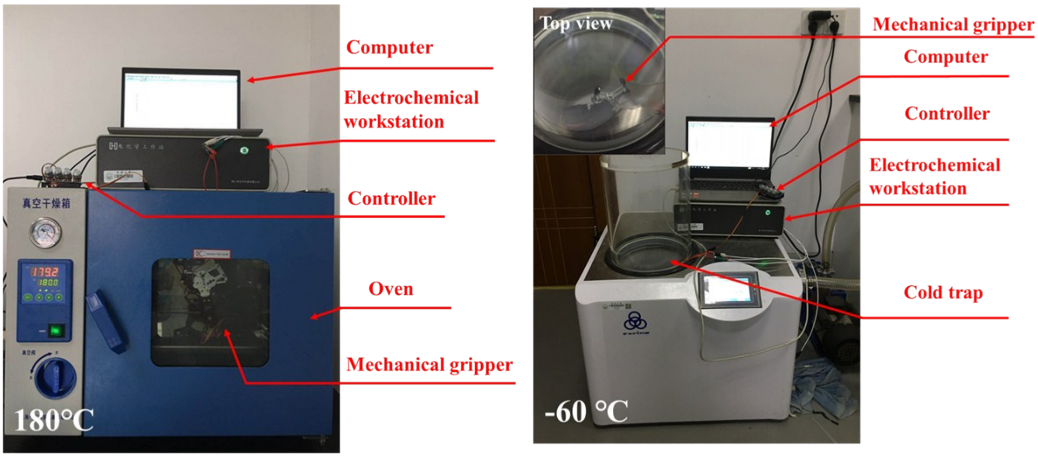

Figure S11. Test system for mechanical grapper behavior detection.

Sol–gel fraction, density and void content

The void content (f_{void}) was calculated as follows:

$$Q_w = (W_{wet} - W_{dry})/W_{dry} \tag{1}$$

The apparent density was calculated as follows:

$$\rho_{app} = W_{dry}/V \tag{2}$$

$$f_{\text{void}} = \frac{\frac{Q_w - 1}{\rho_{Sol}}}{\frac{Q_w - 1}{\rho_{Sol}} + \frac{1}{\rho_{PI}}} \tag{3}$$

Table S1. Density and void content of polyimide organogels

Sample	ρ_{PI} (g/cm^3)	f_{sol} (%)	Q_w (%)	f_{void} (%)
PI-OGel-2wt%	1.35±0.07	0.94±0.0006	17.55±0.18	0.96±0.002
PI-OGel-4wt%	1.33±0.07	0.92±0.0005	11.89±0.07	0.94±0.003
PI-OGel-6wt%	1.36±0.10	0.89±0.0009	9.30±0.08	0.92±0.006
PI-OGel-8wt%	1.35±0.03	0.87±0.0006	7.89±0.04	0.91±0.002

Table S2. Comparison of PI ionogel and other ionogel systems in ionic liquid content (IL content), mechanical properties and conductivity.

System	IL content (wt%)	Tensile stress (MPa)	Tensile strain (%)	Conductivity (mS cm^{-1})	Work Temperature (℃)	reference
BMIMCl/CS/PHEMA Ionogel	80	0.08	~500	23.2	25~200	[1]
PMMA-Silica Nanocomposites Ionogel	76	3.5	200	1.01	N.A.	[2]
Poly(1,2,3-triazolium ionic liquid)s	100	1.2	22	10^{-5}	~200	[3]
PAMPS-based DN Ionogel	66.4	0.38	158	17–24	-70~100	[4]
P(FMA-co-MMA)/P(VDF-co-HFP) DN Ionogel	80	0.66	268	3.3	-40~80	[5]
Pseudo PI Ionogel	75	7.2	12	2.79	25~160	[6]
PI-igels	**85.1-93.1**	**~7.1**	50-320	1.9-5.2	**-60~250**	This work

Reference

(1) Liu, X.; Wen, Z.; Wu, D.; Wang, H.; Yang, J.; Wang, Q. Tough BMIMCl-based ionogels exhibiting excellent and adjustable performance in high-temperature supercapacitors. *Journal of Materials Chemistry A* **2014,** *2* (30), 11569-11573.

(2) Gayet, F.; Viau, L.; Leroux, F.; Mabille, F.; Monge, S.; Robin, J.-J.; Vioux, A. Unique combination of mechanical strength, thermal stability, and high ion conduction in PMMA− Silica nanocomposites containing high loadings of ionic liquid. *Chemistry of Materials* **2009,** *21* (23), 5575-5577.

(3) Obadia, M. M.; Mudraboyina, B. P.; Serghei, A.; Montarnal, D.; Drockenmuller, E. Reprocessing and recycling of highly cross-linked ion-conducting networks through transalkylation exchanges of C–N bonds. *Journal of the American Chemical Society* **2015,** *137* (18), 6078-6083.

(4) Yi, D.; Zhang, J.; Li, C.; Zhang, X.; Liu, H.; Lei, J. Preparation of High-Performance Ionogels with Excellent Transparency, Good Mechanical Strength, and High Conductivity. *Advanced Materials* **2017,** *29* (47), 1704253.

(5) Tang, Z.; Lyu, X.; Xiao, A.; Shen, Z.; Fan, X. High-Performance Double-Network Ion Gels with Fast Thermal Healing Capability via Dynamic Covalent Bonds. *Chemistry of Materials* **2018,** *30* (21), 7752-7759.

(6) Wang, Q.; Jian, Z.; Song, W.-L.; Zhang, S.; Fan, L.-Z. Facile fabrication of safe and robust polyimide fibrous membrane based on triethylene glycol diacetate-2-propenoic acid butyl ester gel electrolytes for lithium-ion batteries. *Electrochimica Acta* **2014,** *149*, 176-185.